



The Dust Deposition Process and Biogeochemical Impacts in the Northern South China Sea

Shuhuan Du^{1,2} · G. M. Ariful Islam^{1,2,3} · Rong Xiang^{1,2} · Xiaoli Yang⁴

Received: 21 July 2019 / Revised: 22 November 2019 / Accepted: 31 December 2019 / Published online: 27 January 2020
© Korean Meteorological Society and Springer Nature B.V. 2020

Abstract

Modern dust plays essential roles in marine sediments, providing nutrient and crucial elements for primary productivity and aquatic ecosystems. However, present marine atmospheric dust observational evidence concerning the biogeochemical response to dust deposition process is spared for a long time. Here a total of 147 aerosols samples were collected near the northern South China Sea (SCS) coast between 13 February, 2016, and 12 February, 2017, have been investigated for the grain size distribution, depositional flux, ten-day back trajectories, clusters analysis, combining with primary productivity (Chlorophyll-a concentration) to indicate the present-day dust deposition process and biogeochemical impacts in the northern SCS on the first time. Our results illustrate the deposition flux and grain size distribution change in different season, grain size distribution in winter are coarser particles than that in the summer, while the maximum and minimum dry deposition flux are 12 December, 2016, ($60.4 \text{ mg m}^{-2} \text{ d}^{-1}$) and 26 August, 2016, ($5 \text{ mg m}^{-2} \text{ d}^{-1}$), respective. In addition, the back trajectories and three clusters analyze results indicating 53% of air masses originating locally near the coastal areas of China from the marine boundary layer (0–0.5 km) in the summer monsoon, while 48% dust from the northeast wind is prevailing during the winter monsoon over a relatively higher level (0–1.5 km). Furthermore, an apparent Chl-a blooming after aeolian dust input with a period of 1–2 days in the SCS. Therefore, atmospheric dust contains readily bioavailable iron and enhance the biogeochemical impact in the oligotrophic SCS.

Keywords Atmospheric dust · Grain size contribution · Deposition flux · Chlorophyll-a concentration · Biogeochemical impacts

1 Introduction

Modern aerosol can affect the climate directly by modifying cloud formations and precipitation processes, while the dust

deposited on the oceans become a significant component of marine sediments, and provide important elements for primary productivity of the marine ecosystem (Duce et al. 1991; Mahowald 2011). Atmospheric inputs such as Fe, Mn, Co, Ni, Cu, and Zn are essential nutrients for marine phytoplankton (Butler 1998; Whitfield 2001), wherein Fe has been suggested as a factor that controls primary productivity in the high-nutrient, low-chlorophyll (HNLC) regions of the ocean (Martin 1990). Dense dust hazes often cover vast areas over the Atlantic, Pacific, and Indian Oceans, with sources in the arid regions of Africa, Asia, and the Middle East. Therefore, in recent times, the influence of aerosols upon coastal and open ocean areas has attracted much attention (Wu et al. 2003; Wong et al. 2007; Ding et al. 2007, 2013; Fu et al. 2011; Wang et al. 2011, 2013; Chuang et al. 2013; Kunwar and Kawamura 2014; Zhao et al. 2016).

However, research on the influence of modern aerosol dust in the South China Sea (SCS), which is the largest marginal sea in China, is still in the initial stages. Furthermore, most of the earlier discussions pertaining to the SCS have focused on the paleoceanographic reconstruction, including the dust

Responsible Editor: Soon-Il An.

Electronic supplementary material The online version of this article (<https://doi.org/10.1007/s13143-019-00171-4>) contains supplementary material, which is available to authorized users.

✉ Shuhuan Du
shuhuandu@scsio.ac.cn

¹ CAS Key Laboratory of Ocean and Marginal Sea Geology, South China Sea Institute of Oceanology, Guangzhou 510301, China

² Innovation Academy of South China Sea Ecology and Environmental Engineering, Chinese Academy of Sciences, Guangzhou 510301, China

³ University of Chinese Academy of Sciences, Beijing 100049, China

⁴ School of Resource Environment and Earth Sciences, Yunnan University, Kunming 650500, China

transport paths (Liu et al. 2014), winter monsoon intensity (Wang et al. 2003), and the connection between dust deposition and primary productivity (Wang et al. 1999). Although the modern dust deposition process and its influence in the SCS have lacked attention till date, the results show its importance and possibilities for further research in the area.

More recently, atmospheric measurements have revealed the possible deposition of long-range transported dust in the northern SCS, and the influence of such dust inputs in the concerned area has attracted scientific interest. In the modern oxidized marine environment, the total surface iron content in the ocean is low, where most of the dissolved iron (Fe^{2+}) can easily and quickly be oxidized to the ferric form, and then transformed into colloidal or particulate iron, which is challenging to be used by the phytoplankton (Rich and Morel 1990). The primary sources of iron in the euphotic layer are (1) dry and wet dust deposits, (2) river input, (3) bottom sediment re-suspension and dissolution (Gerringa et al. 2000). In the coastal estuary area, iron in the surface water comes primarily from the river input, while dust deposit or bottom sediments rework the iron in the open sea (Duce and Tindale 1991; Takeda 1998). According to the research by Li et al. (1985), the amount of surface iron available in the estuarine areas is $29\text{--}1700 \mu\text{g L}^{-1}$, and $0\text{--}54 \mu\text{g L}^{-1}$ in areas away from the coastal zone in the SCS. Similar results of soluble Fe were obtained from the 18°N cross-section in the SCS, with the average soluble Fe being $0.19 \mu\text{g L}^{-1}$ in winter, and $0.17 \mu\text{g L}^{-1}$ in the summertime (South China Sea Ocean Database). These survey data corroborate the findings of numerous earlier studies on the SCS (Gong et al. 1992; Tseng et al. 2005), pointing towards the region's oligotrophic (iron-poor) surface water. Therefore, the terrestrial iron embedded within the dust deposits in this region could be considered as a significant external forcing of the oceanic ecosystem. Wu et al. (2003) speculated that the ecosystem in the SCS is limited by the bioavailability of iron, based on the dissolved inorganic phosphorus concentrations between March and July 2000. Owing to the effective gyration of the basin-wide surface circulations, the lower depths of the SCS is isolated from its surface to become oligotrophic (Gong et al. 1992). Therefore, the atmospheric dust inputs play a significant role in the northern SCS. Atmospheric input could cause chlorophyll distribution response in the ocean, especial in a low-chlorophyll region (Wong et al. 2007). On the global scale, satellite data has often been used to assess the behavior of oceanic biogeochemistry in terms of retrieving information on Chl-a concentration (O'Reilly et al. 1998). In the SCS, the seasonal changes in wind and temperature of the East Asian monsoon, is the primary driving force of ocean current dynamics, mixed layer depth, and upwelling, which in turn influences the chlorophyll distribution in the region (Liu et al. 2002). An observation from SEATS revealed that the seasonal variability of surface Chl-a concentration is related to the

depth of the mixed layer, which is 0.3 mg m^{-3} in winter and 0.03 mg m^{-3} in summer, respectively (Tseng et al. 2005). Even during the wintertime, the survey data of the 18°N cross-section in the SCS also demonstrate low surface Chl-a concentration (0.639 mg m^{-3}) from the South China Sea Ocean DataBase (<http://www.scsio.csdb.cn/>), compared to other marginal seas (Singh et al. 2008), the SCS has been considered a low-chlorophyll region. Therefore, the atmospheric inputs could become an important external forcing of biogeochemistry in the SCS (Wong et al. 2007; Wang et al. 2012).

Hsu et al. (2007) obtained marine aerosols from the area between Taiwan and Dongsha Island, between November 2004 and January 2005, reflecting the different travel histories of the air masses around the SCS coming from anthropogenic sources in the Asian Continent. Hsu et al. (2013) measured the Al concentration during a dust storm event and found that the atmospheric conditions could relatively be more significant than the strength of the dust storm. Similarly, Tan et al. (2012) simulated the total dust deposition during the spring period between 2000 and 2007, and found that the amount of deposition over the northern SCS was three times the deposited amount over the East China Sea. Zhang et al. (2007) collected aerosols from the northern SCS near Hong Kong and the Pearl River estuary in January and April 2003, and observed that Fe (II), which accounts for 16–82% of the total iron in the aerosols, affects the oceanic biogeochemistry. Wang et al. (2012) suggested that the enhanced growth of phytoplankton in the oligotrophic northern SCS is caused by yellow dust (YD) transported from northern China. Wang et al. (2013) observed aerosol particles at Dongsha Island in northern SCS to characterize the source origins, transport processes, and vertical distributions of the Asian continental outflows, based on a yellow-dust event recorded on 21 March 2010. The study suggested that emissions from both China and Southeast Asian countries could have a significant impact on the aerosol loading and other aerosol properties over the SCS. Zhao et al. (2016) collected aerosol samples over the northern SCS from September to October 2013, to analyse the non-polar organic compounds, organic carbon, elemental carbon, and water-soluble ions, and observed that the contributions of continental and oceanic emissions could be categorized into three groups: continental, oceanic, and mixed-influenced.

As a large sink receiving significant amounts of atmospheric dust (Lin et al. 2007; Wang et al. 2011), the aerosol input in the northern SCS has been considered a primary external forcing of this oceanic ecosystem (Wong et al. 2007). Although, aerosol dust is widely recognized as a major contributor and recorder of environmental change, till date, in-depth studies on the current and long-term dust deposition processes in the northern SCS, including studies on the location of the source areas, source-to-sink selective transport processes, the grain

size distribution, deposition flux, chemistry, as well as the biogeochemical response of the marine system to the impact of such atmospheric inputs is scarce. A primary reason for this deficiency could be the difficulty in obtaining long-term and continuous data on atmospheric dust in the open ocean areas, in addition to the lack of connection between long-term aerosol samples and biochemical data in the northern SCS.

In this paper, we discuss a modern dust deposition process and present analyses of the grain size distribution, deposition flux, chemical, and transport paths of aerosols, based on 147 aerosol samples, collected continuously at Shantou near the northern SCS coast from 13 February, 2016 to 12 February, 2017. This paper also discusses the biogeochemical impacts of aerosols over the northern SCS based on analysis of Moderate Resolution Imaging Spectroradiometer (MODIS) derived long-term Chlorophyll-a (Chl-a) concentration data in the region.

2 The Material and Methods

2.1 Sampling

Aerosol samples were collected continuously at Shantou (ST, 23.52° N, 116.80° E) near the northern SCS coast (Fig. 1) during the period from 13 February 2016 to 12 February 2017. A total of 147 total suspended particulate (TSP) samples were collected from the coastal station using a high-volume

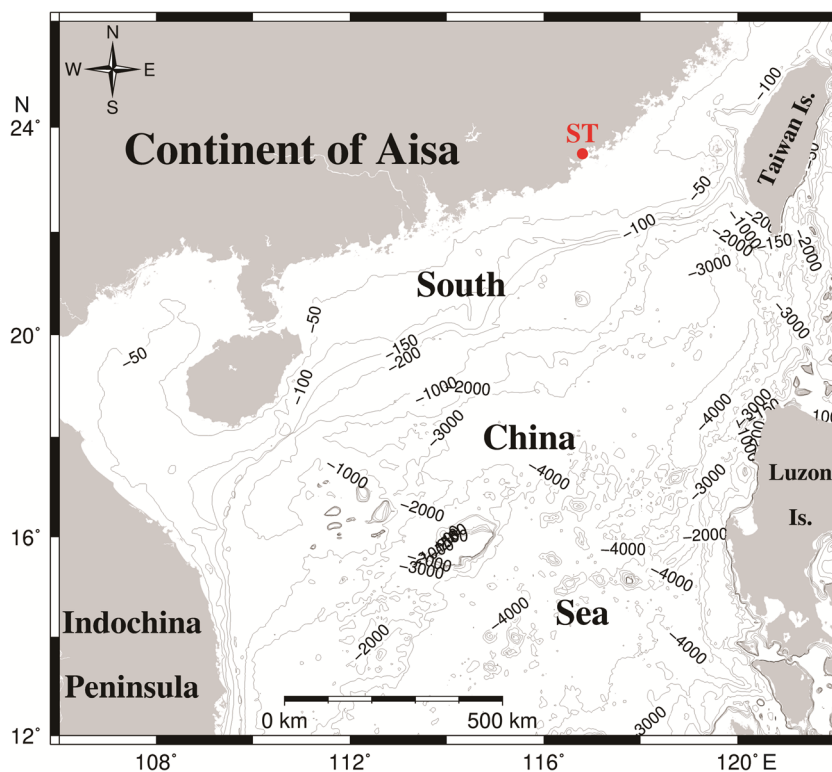
TSP air sampler (KB-100; Qingdao Jinshida Electronic Technology Co. Ltd., China). Each sample was collected over 48 h with a vacuum-cleaner engine, having an air suction rate of $1.05 \text{ m}^3 \text{ min}^{-1}$, through letter-sized ($25 \times 25 \text{ cm}$) glass-fiber filters. The filters were pre-weighed before sample collection and then weighed again after the dust was collected to obtain the dust concentration (C).

The dust samples for analyses were first separated by transferring the filter to glassware containing 20 ml deionized water. This was then vibrated in an ultrasonic cleaner for 15 min, following which the dust particles could be successfully separated repeat two to three times, and were finally collected in a clean beaker. As per the Stokes principle, the samples were allowed to stand for 1–2 days to fully precipitate the dust particles, thereby allowing the dust particles to concentrate and enrich for laboratory analyses.

2.2 Grain Size Analysis

For the grain size analyses, the dust sample was first passed through a $100 \mu\text{m}$ sieve to remove the glass fiber film that might fall off during the separation process. After ultrasonic vibration for laser particle size analyzer measurement. Particle sizes were measured with the Malvern Mastersizer 2000 at the South China Sea Institute of Oceanology, Chinese Academy of Sciences (CAS), which accounts for grains in the $0.02\text{--}2000 \mu\text{m}$ range. The measurement repeatability is 0.5% for a

Fig. 1 The sampling site at Shantou (ST) in the northern South China Sea coastal zone



single sample, and the reproducibility is better than 2% for duplicate samples.

2.3 Dry Deposition Flux

The dry deposition flux (F) of the sample was estimated by multiplying the dust concentration in the TSP sample (C) with dry deposition velocity (V_d). Hence, dust deposition in the northern SCS can be estimated as the dry deposition flux of dust (F), expressed as:

$$F = C \times V_d$$

where C is the dust concentration and V_d is the dry deposition velocity. The dry deposition velocity was assumed to be 2.0 cm s^{-1} , which is consistent with the velocity assumed by Hsu et al. (2009) for Asian dust observed in the East China Sea (ECS).

2.4 Chemical Analysis

Elemental analyses were carried out using an Epsilon 5 high-energy polarized energy-dispersive X-ray fluorescence spectrometer (PANalytical, Netherlands) at the South China Normal University, as per the procedure described by Wen et al. (2016). Concentrations of major and trace elements were simultaneously measured, and the reproducibility was evaluated using the National Standard GSS-17. The precision was better than 5% for the major elements, and 5 to 10% for the trace elements. The major elements were measured and expressed in weight %, while the trace elements were measured and shown in ppm.

2.5 Back Trajectories

Back trajectory data was calculated using the Hybrid Single-Particle Lagrangian Integrated Trajectory (HY-SPLIT4) model developed by the NOAA Air Resources Laboratory (Draxler and Rolph 2003), to analog dust transmission trails at levels that appeared from the daily meteorological data to the ones likely to carry the most material dust loads. From the ARL-NOAA server (<http://www.arl.noaa.gov/ready/hysplit4.html>) to regain the meteorological data and model, while meteorological data obtained from the NCEP Global Data Assimilation System (GDAS) with one-degree resolution to initialize the HY-SPLIT4. Moreover, calculated ten-day back trajectories to cluster analysis (embedded in the HY-SPLIT software), allocating them into groups of similar length, origin, and transit. This model widely used in the modeling and prediction of dust diffusion paths (Waisel et al. 2008).

2.6 Surface Chl-a Concentration

The daily-averaged surface Chl-a concentration for open ocean pixels in the northern SCS was derived from Aqua/MODIS (<https://modis.gsfc.nasa.gov/>). The raw Chl-a data as Level 3 Standard Mapped Images with 9 km resolution were obtained from the NASA/OceanColor website (<http://oceancolor.gsfc.nasa.gov/>). The Matlab software was used to process the data, and all the data on the Chl-a concentration was considered as logarithm with base 10.

3 Results

3.1 Grain Size

The grain size distributions of the aerosol samples ranged from about $0.3\text{--}74 \mu\text{m}$, with more than 85% lying between 0.63 and $20 \mu\text{m}$, the average grain size mode being $\sim 4.7 \mu\text{m}$. Despite a high-frequency variability in the average grain size mode, the grain size results at Shantou exhibited a seasonal distribution trend (Fig. 2a), especially between the different monsoonal current periods (Fig. 2b). Although the aerosol samples from the winter monsoon period of November to April consisted of an average grain size of $4.2 \mu\text{m}$, a similar value of $5.6 \mu\text{m}$ was obtained under the summer monsoon (mid-May to mid-September). As is evident from the different grain size distributions displayed in Fig. 2b, higher sediment peaks occurred during the typical winter monsoon distribution, with the main peak at $\sim 4 \mu\text{m}$, and the second peak at $\sim 0.63 \mu\text{m}$. Similarly, aerosol particles of coarser grain size ($> 11 \mu\text{m}$) were deposited during the given period. On the other hand, the summer monsoon showed a simple distribution mode, with the main peak occurring at $\sim 6 \mu\text{m}$ and low height ($\sim 0.63 \mu\text{m}$) deposited during the typical summer monsoon.

3.2 Dry Deposition Flux

The results obtained from the monthly dry deposition flux and the daily mean of dust particles deposited during different periods are presented in Table 1. The dust flux in the northern SCS coastal zone recorded an average of $35.2 \text{ mg m}^{-2} \text{ d}^{-1}$. However, it exhibited a strong seasonal variability, wherein the winter months exhibited the highest dust flux. A remarkably high flux was recorded for December 2016 at 573.1 mg m^{-2} , with similar high values occurring in January 2017 at 487.7 mg m^{-2} . On the contrary, the dry deposition flux during the summer monsoon showed lower values, such as 256.6 mg m^{-2} in June and 268.9 mg m^{-2} in August. Furthermore, the extreme daily mean dry deposition fluxes occurred during the typical monsoon months, wherein the minimum and maximum daily mean dry deposition fluxes were respectively recorded on

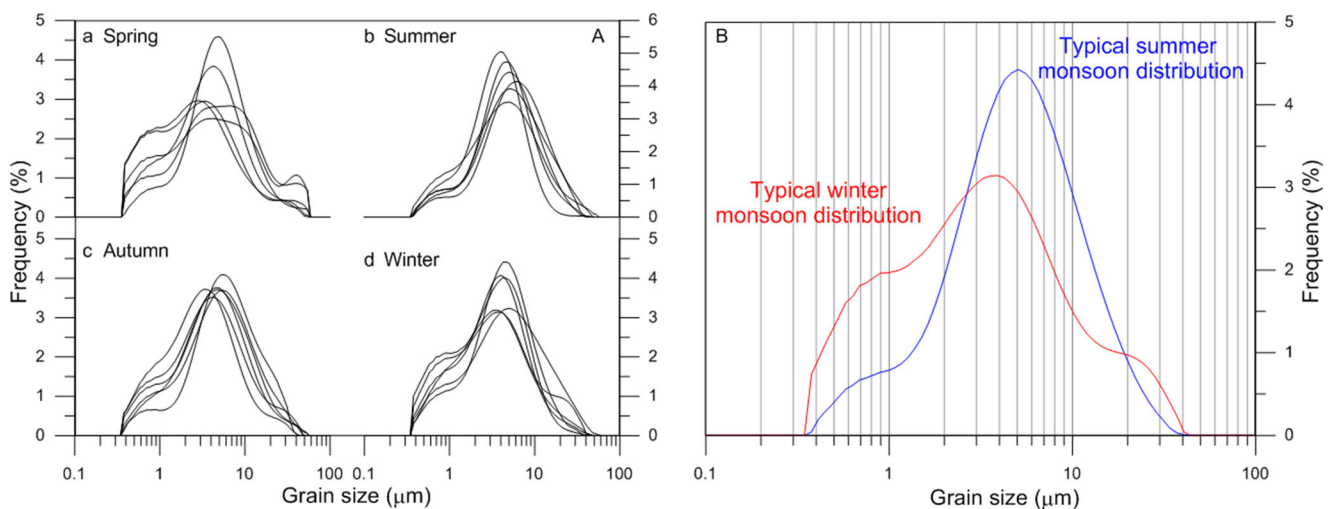


Fig. 2 a. Seasonal grain size distribution, and B. typical monsoonal distribution of aerosol dust deposited at the northern SCS coastal area. The red curve represents a typical winter monsoon distribution, and the blue curve represents a typical summer monsoon distribution

26 August, 2016 (at $5.0 \text{ mg m}^{-2} \text{ d}^{-1}$) and 21 December, 2016 (at $60.4 \text{ mg m}^{-2} \text{ d}^{-1}$).

3.3 Bulk Chemistry

Table 2 summarizes the results of the seasonal bulk chemistry, and the most abundant elements present in aerosols collected over ST were found to be Si, Ca, Al, Mg, and Fe, followed by Zn, Mn, Cu, Ni, and Co in terms of their seasonal mean concentrations. Higher concentrations were observed during winter than summer for the majority of the aerosol elements, such as Fe, Zn, Mn, and Cu, which are essential nutrients for marine phytoplankton, contributed by terrestrial atmospheric inputs. This seasonal variation is consistent with the shift in the prevailing wind direction from the northwest in winter to the south in summer.

3.4 Back Trajectories

Ten-day back trajectories for the aerosol samples in the coastal areas of northern SCS at 0, 1000, and 2000 m levels were

calculated under different prevailing wind conditions (Fig. 3a, c). The differences in the back trajectories between the summer monsoon and winter monsoon are highlighted. The transport paths during the summer period originate from the ocean and are modified by the marine environment, while during the winter monsoon, the northeast winds drive the aeolian dust transport. The cluster analysis results (Fig. 4) show the path with different occurrence percentage of the backward trajectories. Three clusters (Clusters 1–3) were identified in the summer monsoon (Fig. 4a, i.e., 26 August 2016) and winter monsoon (Fig. 4b, i.e., 21 December 2016).

3.5 Surface Chl-a Concentration

The mean surface Chl-a concentration (mg m^{-3}) maps based on the available composited Aqua/ MODIS seasonal data sets between 10 and 25° N , and 105 – 125° E of the SCS are shown in Fig. 5. As shown in Fig. 5, summer monsoon (summer and autumn combined) with lower Chl-a concentration than that in the winter monsoon (spring and winter). Similar notable variation was found in the daily mean surface Chl-a concentration

Table 1 The monthly dry deposition flux and daily mean of dust particles in different periods

Sample periods	Monthly/ $\text{mg m}^{-2} \text{ month}^{-1}$ (daily)/ $\text{mg m}^{-2} \text{ d}^{-1}$	Sample periods	Monthly/ $\text{mg m}^{-2} \text{ month}^{-1}$ (daily)/ $\text{mg m}^{-2} \text{ d}^{-1}$
2016/2/13—2016/2/29	222.5 (24.7)	2016/9/1—2016/9/30	323.8 (23.1)
2016/3/1—2016/3/31	484.5 (31.2)	2016/10/1—2016/10/31	325.8 (23.2)
2016/4/1—2016/4/30	362.0 (25.9)	2016/11/1—2016/11/30	403.8 (31.1)
2016/5/1—2016/5/31	282.0 (20.1)	2016/12/1—2016/12/31	573.1 (40.9)
2016/6/1—2016/6/30	256.6 (18.2)	2017/1/1—2017/1/31	487.7 (34.8)
2016/7/1—2016/7/31	354.3 (25.3)	2017/2/1—2017/2/12	119.9 (30.0)
2016/8/1—2016/8/31	268.9 (19.2)		

Table 2 Seasonal elements of atmospheric dust in the northern coastal zone of SCS

Element Period	SI		CA		AL		MG		FE		ZN		CD	
	NET. (CPS/MA)	CONC. (%)	NET. (CPS/MA)	CONC. (%)	NET. (CPS/MA)	CONC. (%)	NET. (CPS/MA)	CONC. (%)	NET. (CPS/MA)	CONC. (%)	NET. (CPS/MA)	CONC. (PPM)	NET. (CPS/MA)	CONC. (PPM)
Summer	37.8	21.5	1124.3	9.6	8.4	2.2	0.67	1.9	267.6	0.9	418.0	996.0	1.69	0.68
Winter	26.6	16.8	803.9	7.2	6.2	0.7	0.47	1.3	284.6	1.0	395.7	1001.6	0.95	0.40
Element Period	MN		CU		NI		CO		AS		PB		CR	
Summer	10.2	321	10.0	32.0	5.2	28.5	0.44	0.5	14.0	32.6	14.8	48	1.26	45
Winter	10.7	337	29.1	98.6	3.9	27.6	0.45	0.5	12.6	28.4	13.6	47	1.32	37

between the summer (e.g., August 26) and the winter monsoons (e.g., December 21), with much higher density during the latter (Fig. 3d) than the former (Fig. 3b).

4 Discussion

The results of the backward trajectories analyses indicate three clusters (Clusters 1–3) under different monsoon seasons (Fig. 4). The central trajectories cluster shows the occurrence percentage of path ending at the ground level of ST during the summer (26 August 2016, Fig. 4a) and winter monsoons (21 December 2016, Fig. 4b), whereas individual trajectories represent each path and corresponding occurrence percentage. Hence it can be assumed that the air quality at ST is directly related to the monsoon wind across the SCS. From the cluster analysis of 26 August, it was observed that Cluster 3 accounts for 53% of air masses originating locally near the coastal areas of China (Fig. 4a). The path of these trajectories arose from the marine boundary layer (0–0.5 km) modified by the marine environment. Both Clusters 1 and 2 (15% and 33% respectively) reflect air masses, having traversed south-westward from the SCS, all of them exhibit variability concerning transport within the 500 m altitude, accompanied by the dominant wind across the SCS in the summer monsoon (Wang et al. 2003). The dust from the Gobi desert can be considered negligible, whereas the densely populated and industrialized areas in Southeast Asia could have a significant impact on the air mass depositing over the SCS (Lin et al. 2007; Wang et al. 2011). In contrast, trajectories of the winter monsoon indicate different backward paths and heights on 21 December 2016. The maximum ratio of Cluster 1 (48%) comes from the northeast wind prevailing under the winter monsoon (Wang et al. 2003), which is similar to the summer monsoon along with the coastal areas of China, but over a relatively higher level (0–1.5 km). Both the other two paths originate from the central Asian continent, although in different directions and altitudes (Fig. 4b). Cluster 2 consists of trajectories primarily confined to below 3 km, while Cluster 3 reveals trajectories at higher than 6 km and over longer distances. Cluster analysis results indicated that the air mass from the Asian area mainly controls dust transport and deposition in the SCS during the winter period.

These findings suggest that the dust transport paths in the northern SCS depend on the East Asian monsoon (Wang et al. 1999; Hsu et al. 2013; Chuang et al. 2013; Liu et al. 2015), wherein air masses from various sources, transported at varying atmospheric levels and directions, could be responsible for the variation in the grain size distributions, dust flux, and elemental composition. There are three frequency peaks in the grain size mode of the winter season compared to the two peaks in the summer mode, while the different dust

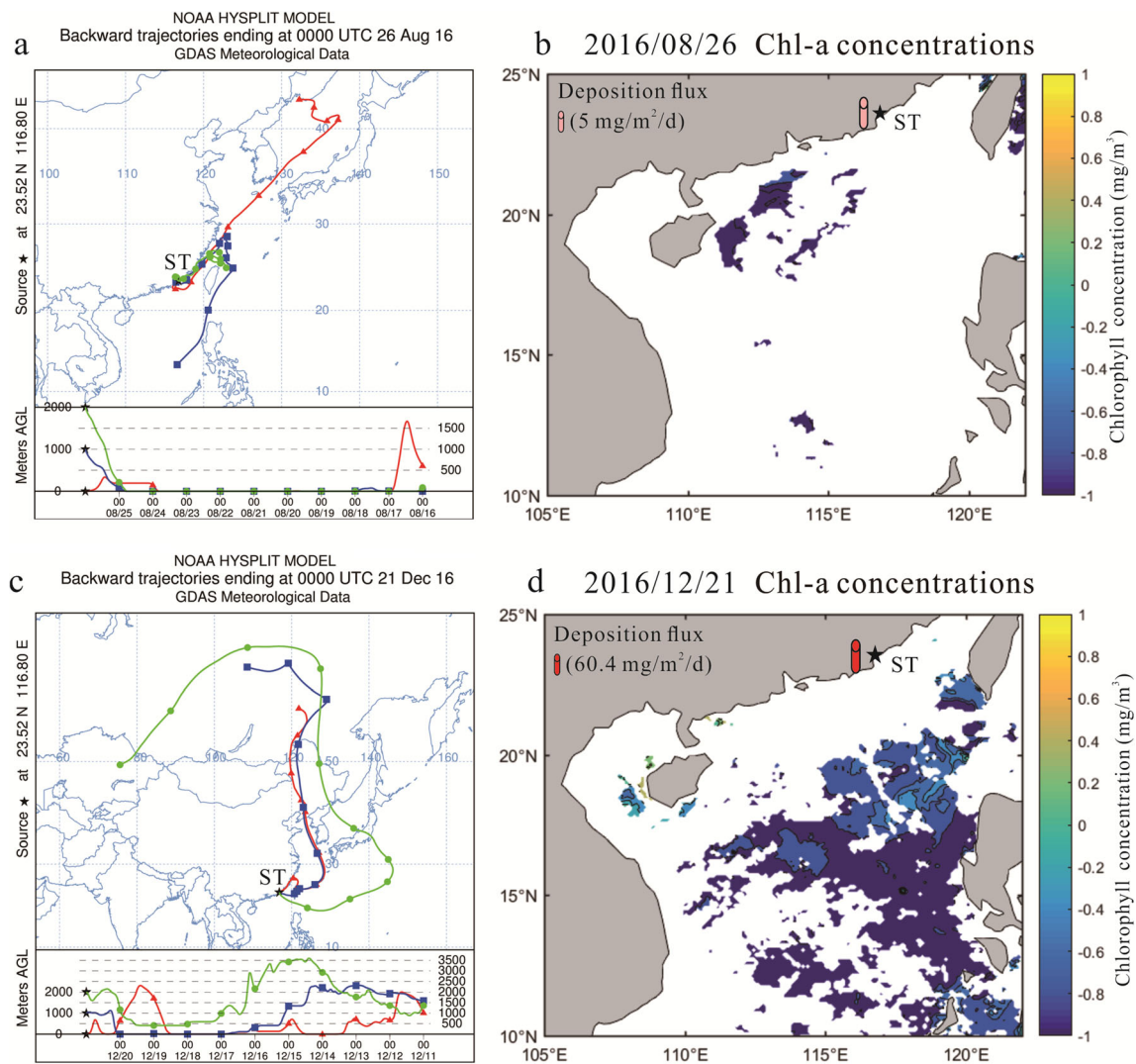


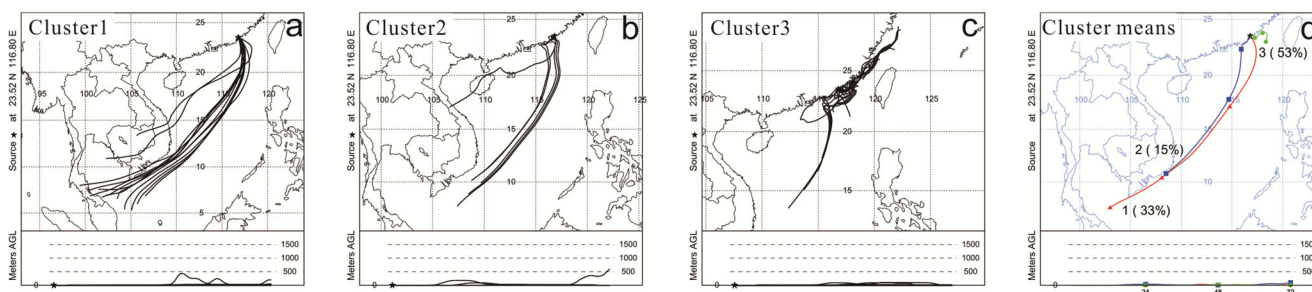
Fig. 3 Ten-day backward trajectory simulated by HY-SPLIT 4 (HY-SPLIT model available from NOAA Air Resources Laboratory and Display system at <http://www.arl.noaa.gov/ready/hysplit4.html>) under different prevailing monsoon months, and the corresponding daily Chl-

a concentration (mg m^{-3}) data derived from Aqua/MODIS. **a**, the backward trajectory and **b**, Chl-a concentration on 26 August, 2016; **c**, the backward trajectory and **b**, Chl-a concentration on 21 December, 2016

transport paths and levels cause both finer materials ($0.63 \mu\text{m}$) and coarser particles in the former than in the latter (Figs. 2 and 4). It is interesting to note that the dust flux in the study area reveals a substantial seasonal variability. Winter has the highest dust flux ($\sim 1403 \text{ mg m}^{-2}$), and a remarkable contribution to the daily flux (maximum of $60.4 \text{ mg m}^{-2} \text{ d}^{-1}$ on 21 December 2016). Similar values of dust flux were estimated in spring ($\sim 1129 \text{ mg m}^{-2}$) and autumn ($\sim 1053 \text{ mg m}^{-2}$). The dust flux in summer showed the lowest value ($\sim 880 \text{ mg m}^{-2}$), with the minimum daily dust flux occurrence on 26 August 2016 ($5.0 \text{ mg m}^{-2} \text{ d}^{-1}$). Seasonal aerosol flux change in the northern SCS coastal zone leads to different mean surface Chl-a concentration reconstruction based on the Aqua/MODIS (Fig. 5), with lower Chl-a concentration in the summer monsoon (summer and autumn combined) than in the winter monsoon (spring and winter). Model results suggested that pyrogenic

Fe substantially contributes to total aerosol Fe over the northern South China Sea (Ito et al. 2019). The back trajectories indicate different originating sources of the dust between summer monsoon and winter monsoon, wherein more terrestrial air particles are transported to the northern SCS coastal zone during the wintertime, compared to the southwesterly winds prevailing during summer. These results have important implications suggesting that much of the terrestrial elements embedded in the mineral dust are transported over long distances before reaching the northern SCS. The essential nutrients element in the transported dust (such as Fe, Zn, Mn, and Cu) are higher in winter than in summer (Table 2), and are relevant to the marine primary productivity in the ocean (Martin 1990; de Baar 1990; Bruland 1989; Paytan et al. 2009; Jordi et al. 2012). Iron is crucial for phytoplankton growth, being necessary for electron transport, oxygen metabolism, nitrogen

A. The paths with occurrence percentage of backward trajectories ending at ST on 26 August, 2016



B. The paths with occurrence percentage of backward trajectories ending at ST on 21 December, 2016

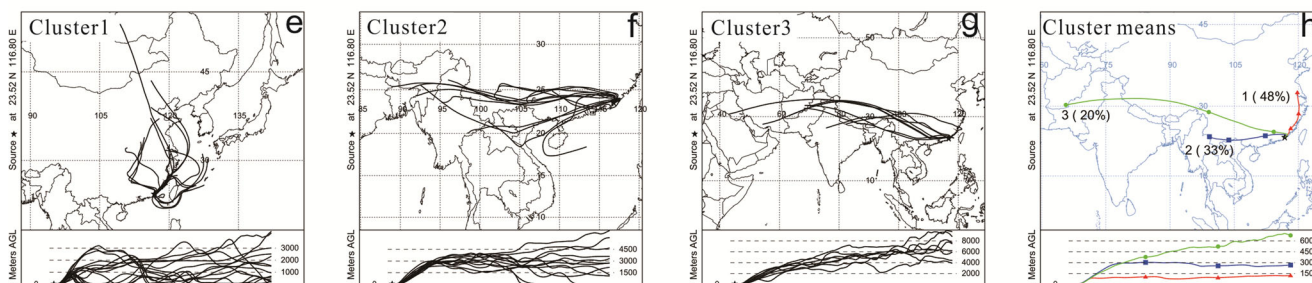


Fig. 4 HY-SPLIT cluster plots for backward trajectories ending at the ground level of ST. A. as on 26 August, 2016, and B. as on 21 December, 2016

absorption and utilization, chlorophyll photosynthesis, and respiration (Flynn and Hipkin 1999; Geider 1999).

Singh et al. (2008) used Aqua/MODIS data and found that a time-lag in chlorophyll blooming responds to aeolian dust input over a period of 1–2 to up to 3–4 days in the Arabian Sea. Wang et al. (2012) investigated dust transport by using a combination of satellite imagery and surface PM_{10} observations, and found that heavy Asian dust events contain significant fractions of bioavailable iron, and Chl-a concentration was significantly enhanced in response to the passage of these airborne dust plumes, especially in the slope area susceptible to dust fertilization and trigger phytoplankton blooms.

Analyses of the dust deposition flux in the study area and the corresponding mean surface Chl-a concentration based on the available Aqua/MODIS data revealed the biogeochemical impacts of atmospheric dust inputs in the SCS, and an apparent surface Chl-a concentration-response during different monsoon periods. During the summer monsoon, most of the dust is transported by the southwest wind from the ocean (Fig. 3a), and the dust deposition flux on the surface water ($\sim 880 \text{ mg m}^{-2}$) is too low to affect the surface Chl-a concentration. The minimum daily dry dust deposition flux on 26 August at ST ($5.0 \text{ mg m}^{-2} \text{ d}^{-1}$) corresponded to a small quantity of surface Chl-a concentration (Fig. 3b). However, the maximum daily dry dust deposition in the study area on 21 December at $60.4 \text{ mg m}^{-2} \text{ d}^{-1}$ indicated substantial dust input in the SCS within 48 h from the Asian continent. This dust had been transported over long distances and contained higher essential nutrients elements, which

could contribute to a positive Chl-a anomaly (Fig. 4d) in the study area. Consequently, the northern SCS coastal zone receives dust over different seasons and from different directions, laden with various terrestrial nutrients elements (like Fe), thereby causing sensitive biogeochemical impacts in the northern SCS.

5 Conclusions

In this study, we investigated the grain size distribution, depositional flux, ten-day backward trajectories, and cluster analysis, and primary productivity (in terms of Chl-a concentration) of atmospheric dust collected over a year's time near the northern SCS coastal zone, to assess the current dust deposition processes and their biogeochemical impacts in the northern SCS. The grain size analysis of 147 atmospheric dust samples at ST showed that the grain size distribution varies between the typical winter and summer monsoons, with the particles being coarser in winter than in summer. Likewise, the grain size mode displayed a higher frequency of peaks in winter (three) compared to that in summer (two), which indicates a clear seasonal variability trend. Similar findings have been reported elsewhere for dry dust flux. Winter displayed the highest dust flux ($\sim 1403 \text{ mg m}^{-2}$) compared to summer (lowest at $\sim 880 \text{ mg m}^{-2}$), with the extreme daily fluxes recorded on 21 December ($60.4 \text{ mg m}^{-2} \text{ d}^{-1}$) and 26 August ($5.0 \text{ mg m}^{-2} \text{ d}^{-1}$).

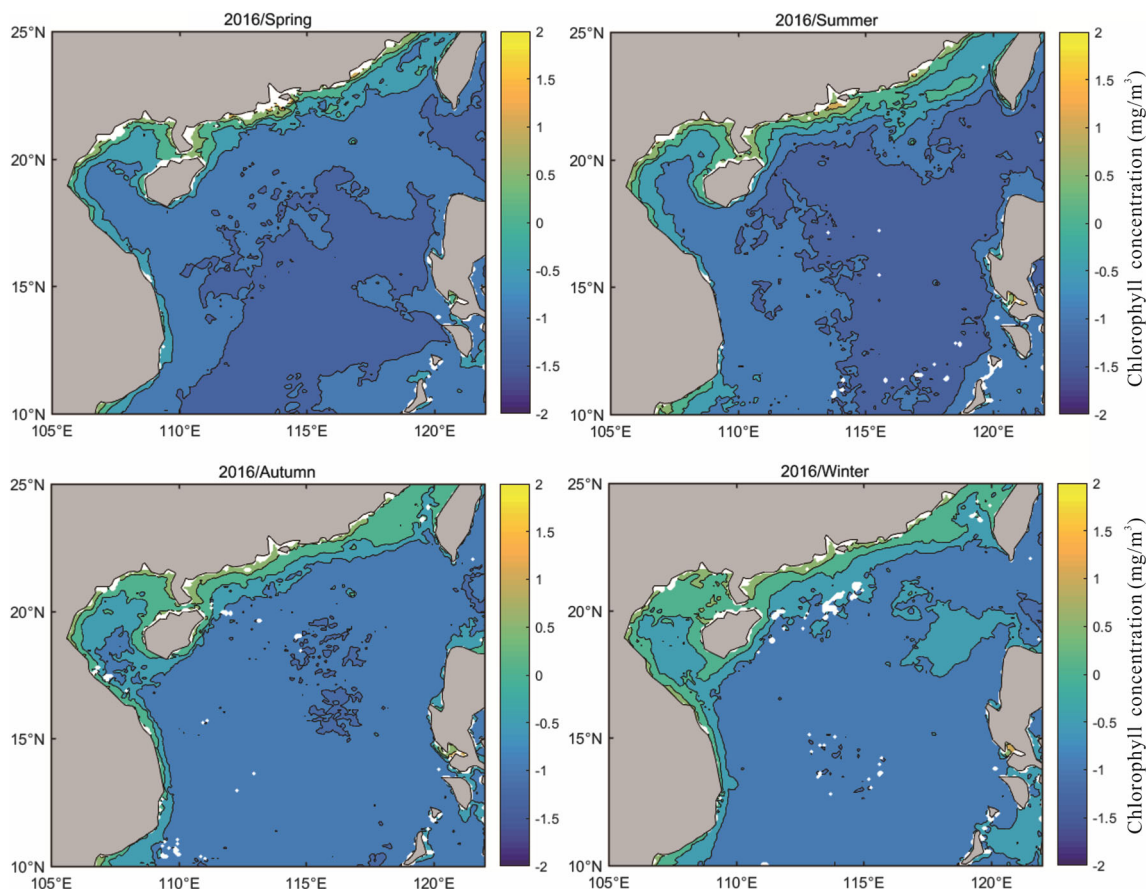


Fig. 5 Seasonal mean surface Chl-a concentration (mg m^{-3}) based on the available composited Aqua/MODIS data sets between 10 and 25° N and 105–125° E from the SCS

These seasonal differences are closely linked to the dust transport paths and respond to the air masses originating from various sources and transported at different atmospheric levels in different directions. The results of the ten-day back trajectories analysis and the three clusters obtained during the summer monsoon indicate that 53% of the air masses originate locally from the marine boundary layer (0–0.5 km) near the coastal areas of China. Along with this, the prevailing southwestward wind across the SCS in the summer monsoon exhibit variability in transport within 500 m altitudes. In contrast, the maximum ratio of Cluster 1 (48%) comes from the northeast wind prevailing over a relatively higher level (0–1.5 km) during the winter monsoon, while both the other two paths originate from the central Asian continent, though in different directions and altitudes. The transport and input of higher dust flux composed of terrestrial elements in the ocean can be considered to be a major external forcing of the oceanic ecosystem in the oligotrophic (iron-poor) surface water of the SCS.

The remarkable dust input in the northern SCS over 48 h, transported over long distances from the Asian continent, and constituted of higher amounts of essential nutrients elements, led to a positive Chl-a anomaly on 21 December, 2016. Contrary to the low value of dust flux deposit on 26 August, the dust flux in December triggered

phytoplankton blooms in the otherwise oligotrophic northern SCS. Hence, atmospheric dust laden with various terrestrial elements (such as Fe) deposited during different seasons and directions display sensitive biogeochemical response in the northern SCS.

Acknowledgments This work was funded by the Guangdong Province Science and Technology Project (No. 2015A020216015), Natural Science Foundation of Guangdong Province (No. 2018A0303130 156) and Innovative Development Fund projects of Innovation Research Institute on the South China Sea Ecological and Environmental Engineering, Chinese Academy of Sciences (No. ISEE2018PY02). We also acknowledge for the data support from “South China Sea and Adjacent Seas Data Center, National Earth System Science Data Sharing Infrastructure, National Science & Technology Infrastructure of China. (<http://ocean.geodata.cn>).

References

- Bruland, K.W.: Complexation of zinc by natural organic ligands in the central North Pacific. *Limnol. Oceanogr.* **34**, 269–285 (1989)
- Butler, A.: Acquisition utilization of transition metal ions by marine organisms. *Science*. **281**, 207–209 (1998)
- Chuang, M.T., Chang, S.C., Lin, N.H., Wang, J.L., Sheu, G.R., Chang, Y.J., Lee, C.T.: Aerosol chemical properties and related pollutants

- measured in Dongsha Island in the northern South China Sea during 7-seas/Dongsha experiment. *Atmos. Environ.* **78**, 82–92 (2013)
- de Baar, H.J.: On Iron limitation of the Southern Ocean: experimental observations in the Weddell and scotia seas. *Mar. Ecol. Prog. Ser.* **65**, 105–122 (1990)
- Ding, X., Wang, X.-M., Xie, Z.-Q., Xiang, C.-H., Mai, B.-X., Sun, L.-G., Zheng, M., Sheng, G.-Y., Fu, J.-M., Pöschl, U.: Atmospheric polycyclic aromatic hydrocarbons observed over the North Pacific Ocean and the Arctic area: spatial distribution and source identification. *Atmos. Environ.* **41**, 2061–2072 (2007)
- Ding, X., Wang, X., Xie, Z., Zhang, Z., Sun, L.: Impacts of Siberian biomass burning on organic aerosols over the North Pacific Ocean and the Arctic: primary and secondary organic tracers. *Environ. Sci. Technol.* **47**, 3149–3157 (2013)
- Draxler, R.R., Rolph, G.D.: HYSPLIT (Hybrid Single-Particle Lagrangian Inter-grated Trajectory) Model Access via NOAA ARL READY Website. NOAA AIR Resources Laboratory, Silver Spring, MD. <http://www.arl.noaa.gov/ready/hysplit4.html> (2003)
- Duce, R.A., Tindale, N.W.: Atmospheric transport of Iron and its deposition in the ocean. *Limnol. Oceanogr.* **36**, 1715–1726 (1991)
- Duce, R., Liss, P., Merrill, J., Atlas, E., Buat-Menard, P., Hicks, B., Miller, J., Prospero, J., Arimoto, R., Church, T.: The atmospheric input of trace species to the World Ocean. *Global Biogeochem. Cy.* **5**, 193–259 (1991)
- Flynn, K. J., Hipkin, C. R.: Interactions between iron, light, ammonium, and nitrate: insights from the construction of a dynamic model of algal physiology. *Journal of Phycology* **35**:1171–1190 (1999)
- Fu, P., Kawamura, K., Miura, K.: Molecular characterization of marine organic aerosols collected during a round-the-world cruise. *J. Geophys. Res.-Atmos.* **116**, D13302 (2011). <https://doi.org/10.1029/2011JD015604>
- Geider, R.J.: Biological oceanography: complex lessons of iron uptake. *Nature* **400**: 815–816 (1999)
- Gerringa, L.J.A., de Baar, H.J.W., Timmermans, K.R.: A comparison of iron limitation of phytoplankton in natural oceanic waters and laboratory media conditioned with EDTA. *Mar. Chem.* **68**, 335–346 (2000)
- Gong, G.-C., Liu, K.K., Liu, C.-T., Pai, S.-C.: The chemical hydrography of the South China Sea west of Luzon and a comparison with the west Philippine Sea. *Terr. Atmos. Ocean. Sci.* **3**, 587–602 (1992)
- Hsu, S.C., Liu, S.C., Kao, S.J., Jeng, W.L., Huang, Y.T., Tseng, C.M., Tsai, F., Tu, J.Y., Yang, Y.: Water-Soluble Species in the Marine Aerosol from the Northern South China Sea: High Chloride Depletion Related to Air Pollution. *J. Geophys. Res.-Atmos.* **112**, D19304 (2007). <https://doi.org/10.1029/2007JD008844>
- Hsu, S.C., Liu, S.C., Arimoto, R., Liu, T.H., Huang, Y.T., Tsai, F., Lin, F.J., Kao, S.J.: Dust Deposition to the East China Sea and Its Biogeochemical Implications. *J. Geophys. Res.-Atmos.* **114**, D15304 (2009). <https://doi.org/10.1029/2008JD011223>
- Hsu, S.C., Tsai, F., Lin, F.J., Chen, W.N., Shiah, F.K., Huang, J.C., Chan, C.Y., Chen, C.C., Liu, T.H., Chen, H.Y.: A super Asian dust storm over the east and South China seas: disproportionate dust deposition. *J. Geophys. Res.-Atmos.* **118**, 7169–7181 (2013)
- Ito, A., Myriokefalitakis, S., Kanakidou, M., Mahowald, N.M., Scanza, R.A., Hamilton, D.S., Baker, A.R., Jickells, T., Sarin, M., Bikkina, S., Gao, Y., Shelley, R.U., Buck, C.S., Landing, W.M., Bowie, A.R., Perron, M.M.G., Guieu, C., Meskhidze, N., Johnson, M.S., Feng, Y., Kok, J.F., Nenes, A., Duce, R.A.: Pyrogenic iron: The missing link to high iron solubility in aerosols. *Sci. Adv.* **5**(5), eaau7671 (2019). <https://doi.org/10.1126/sciadv.aau>
- Jordi, A., Basterretxea, G., Tovar-Sánchez, A., Alastuey, A., Querol, X.: Copper aerosols inhibit phytoplankton growth in the Mediterranean Sea. *P. Natl Acad. Sci. USA.* **109**, 21246–21249 (2012)
- Kunwar, B., Kawamura, K.: One-year observations of carbonaceous and nitrogenous components and major ions in the aerosols from subtropical Okinawa Island, an outflow region of Asian dusts. *Atmos. Chem. Phys.* **14**, 1819–1836 (2014)
- Li, P.C., Han, W.Y., Huang, X.N.: Distribution of iron in the seawater of the northeastern South China Sea. *Trop. Oceanol.* **4**(4), 77–82 (1985)
- Lin, I., Chen, J.P., Wong, G.T., Huang, C.W., Lien, C.C.: Aerosol input to the South China Sea: results from the moderate resolution imaging Spectro-radiometer, the quick Scatterometer, and the measurements of pollution in the troposphere sensor. *Deep-Sea Res. PT II.* **54**, 1589–1601 (2007)
- Liu, K.K., Chao, S.Y., Shaw, P.T., Gong, G.C., Chen, C.C., Tang, T.Y.: Monsoon-forced chlorophyll distribution and primary production in the South China Sea: Observations and a numerical study. *Deep-Sea Res. PT I.* **49**(8), 1387–1412 (2002)
- Liu, Y., Sun, L., Zhou, X., Luo, Y., Huang, W., Yang, C., Wang, Y., Huang, T.: A 1400-year terrigenous dust record on a Coral Island in South China Sea. *Sci. Rep.* **4**, 4994 (2014)
- Liu, Y., Sun, L.G., Zhou, X., Luo, Y.H.: Wen Huang, Chengyun Yang, Yuhong Wang and Tao Huang, A 1400-year terrigenous dust record on a coral island in South China Sea. *Sci. Rep.* **4**: 1 (2015)
- Mahowald, N.: Aerosol indirect effect on biogeochemical cycles and climate. *Science.* **334**, 794–796 (2011)
- Martin, J.H.: Glacial-interglacial Co₂ change: the Iron hypothesis. *Paleoceanography.* **5**, 1–13 (1990)
- O'Reilly, J.E., Maritorena, S., Mitchell, B.G., Siegel, D.A., Carder, K.L., Garver, S.A., Kahru, M., McClain, C.: Ocean color chlorophyll algorithms for SeaWiFS. *J. Geophys. Res.* **103**(C11), 24937–24953 (1998). <https://doi.org/10.1029/98JC02160>
- Paytan, A., Mackey, K.R., Chen, Y., Lima, I.D., Doney, S.C., Mahowald, N., Labiosa, R., Post, A.F.: Toxicity of atmospheric aerosols on marine phytoplankton. *P. Natl Acad. Sci. USA.* **106**, 4601–4605 (2009)
- Rich, H.W., Morel, F.M.: Availability of well-defined Iron colloids to the marine diatom *Thalassiosira weissflogii*. *Limnol. Oceanogr.* **35**, 652–662 (1990)
- Singh, R.P., Prasad, A.K., Kayetha, V.K., Kafatos, M.: Enhancement of oceanic parameters associated with dust storms using satellite data. *J. Geophys. Res.* **113**, C11008 (2008). <https://doi.org/10.1029/2008JC004815>
- Takeda, S.: Influence of Iron availability on nutrient consumption ratio of diatoms in oceanic waters. *Nature.* **393**, 774 (1998)
- Tan, S.C., Shi, G.Y., Wang, H.: Long-range transport of spring dust storms in Inner Mongolia and impact on the China seas. *Atmos. Environ.* **46**, 299–308 (2012)
- Tseng, C.M., Wong, G.T.F., Lin, I.I., Wu, C.R., Liu, K.K.: A unique seasonal pattern in phytoplankton biomass in low-latitude waters in the South China Sea. *Geophys. Res. Lett.* **32**, L08608 (2005). <https://doi.org/10.1029/2004GL022111>
- Waisel, Y., Ganor, E., Epshtein, V., Stupp, A., Eshel, A.: Airborne pollen, spores, and dust across the East Mediterranean Sea. *Aerobiologia.* **24**, 125–131 (2008)
- Wang, L., Sarnthein, M., Erlenkeuser, H., Grimalt, J., Grootes, P., Heilig, S., Ivanova, E., Kienast, M., Pelejero, C., Pflaumann, U.: East Asian monsoon climate during the Late Pleistocene: high-resolution sediment records from the South China Sea. *Mar. Geol.* **156**, 245–284 (1999)
- Wang, B., Clemens, S.C., Liu, P.: Contrasting the Indian and east Asian monsoons: implications on geologic timescales. *Mar. Geol.* **201**, 5–21 (2003)
- Wang, S.H., Tsay, S.C., Lin, N.H., Hsu, N.C., Bell, S.W., Li, C., Ji, Q., Jeong, M.-J., Hansell, R.A., Welton, E.J.: First detailed observations of long-range transported dust over the northern South China Sea. *Atmos. Environ.* **45**, 4804–4808 (2011). <https://doi.org/10.1016/j.atmosenv.2011.04.077>
- Wang, S.H., Hsu, N.C., Tsay, S.C., Lin, N.H., Sayer, A.M., Huang, S.J., Lau, W.K.M.: Can Asian dust trigger phytoplankton blooms in the

- oligotrophic northern South China Sea? *Geophys. Res. Lett.* **39**, L05811 (2012). <https://doi.org/10.1029/2011GL050415>
- Wang, S.H., Tsay, S.C., Lin, N.H., Chang, S.C., Li, C., Welton, E.J., Holben, B.N., Hsu, N.C., Lau, W.K., Lolli, S.: Origin, transport, and vertical distribution of atmospheric pollutants over the northern South China Sea during the 7-seas/Dongsha experiment. *Atmos. Environ.* **78**, 124–133 (2013)
- Wen, X.H., Li, B.S., Zheng, Y.M., Yang, Q.J., Niu, D.F., Shu, P.X.: Early Holocene multi-centennial moisture change reconstructed from lithology, grain-size and chemical composition data in the eastern Mu Us desert and potential driving forces. *Palaeogeography, Palaeoclimatology, Palaeoecology* **459**:440–452 (2016)
- Whitfield, M.: Interactions between phytoplankton and trace metals in the ocean. *Adv. Mar. Biol.* **41**, 1–128 (2001)
- Wong, G.T., Ku, T.L., Mulholland, M., Tseng, C.M., Wang, D.P.: The southeast Asian time-series study (Seats) and the biogeochemistry of the South China Sea—an overview. *Deep-Sea Res. PT II.* **54**, 1434–1447 (2007)
- Wu, J., Chung, S.W., Wen, L.S., Liu, K.K., Chen, Y.L.L., Chen, H.Y., Karl, D.M.: Dissolved Inorganic Phosphorus, Dissolved Iron, and Trichodesmium in the Oligotrophic South China Sea. *Global Biogeochem. Cy.* **17**, 8-1-8-10 (2003)
- Zhang, X.Y., Zhuang, G.S., Guo, J.H., Yin, K.D., Zhang, P.: Characterization of aerosol over the Northern South China Sea during two cruises in 2003. *Atmospheric Environment* **41**:7821–7836 (2007)
- Zhao, Y., Zhang, Y., Fu, P., Ho, S.S.H., Ho, K.F., Liu, F., Zou, S., Wang, S., Lai, S.: Non-polar organic compounds in marine aerosols over the northern South China Sea: influence of continental outflow. *Chemosphere.* **153**, 332–339 (2016)

Publisher's Note Springer Nature remains neutral with regard to jurisdictional claims in published maps and institutional affiliations.

